Stefanovic, C., et al. On the second order statistics of N-Hop FSO communications over N-gamma-gamma turbulence induced fading channels, In: *Physical Communication, Vol. 45, April 2021, 101289, 11 pp.*

DOI: https://doi.org/10.1016/j.phycom.2021.101289

On the Second Order Statistics of *N*-Hop FSO Communications over *N*-Gamma-Gamma Turbulence Induced Fading Channels

Časlav Stefanović[a,*,1], Stefan Panić[b], Danijel Djosić[b], Dejan Milić[c], Mihajlo Stefanović[c]

[a]Universidad Carlos III de Madrid, Department of Signal Theory and Communications, 28911 Leganés, Spain

[b]University of Pristina, Faculty of Sciences and Mathematics, Kosovska Mitrovica, Serbia

[c]University of Nis, Faculty of Electronic Engineering, Nis, Serbia

*Corresponding author: Caslav Stefanovic

[1]Caslav Stefanovic was previously with University of Pristina, Faculty of Sciences and Mathematics, Kosovska Mitrovica, Serbia.

Abstract

The paper explores *N*-hop FSO communications assisted by amplify-and-forward relays (AFRs) over *N*-gamma-gamma (*N*-gg) turbulence induced (TI) fading channels. We model TI fading signal as the product of independent but not necessarily identically distributed (i.n.i.d) *N* number of gg random processes (RPs) in order to address *N*-hop AFR FSO communications in moderate to strong TI fading conditions. The closed form statistical measures such as: probability density function (PDF), cumulative distribution function (CDF), average level crossing rate (LCR) and average fade duration (AFD) approximated by general Laplace integration formula (LIF) and exponential LIF are derived. The CDF and AFD derived expressions are in terms of finite sums and valid only for an integer value of the parameter related to small-scale atmospheric cells in the first link of *N*-hop AFR FSO system. The numerical examples for moderate to strong TI fading conditions as well as for various number of hops for the proposed *N*-hop AFR FSO systems are presented and discussed. Moreover, LIF approximate numerical results are compared with numerical results evaluated from exact integral expressions for the observed system model parameters.

Keywords: FSO, Gamma-gamma, Laplace approximation, multi-hop relaying, second order statistics.

1. Introduction

Free space optical (FSO) communications re-present promising solution for integration in future 5G and beyond 5G (B5G) communication systems [1]-[4]. The FSO links are mainly applied to increase data rate and provide wider bandwidth in comparison to existing radio-frequency (RF) communications. An FSO link is spectrum license free. Moreover, FSO links can provide cost effective solutions and annulate the impact of channel interference. The main cause of FSO system performance deterioration is turbulence induced (TI) fading due to the existence of small- and large-scales atmospheric cells. Moreover, atmospheric conditions (such as fog, rain and etc.) as well as pointing errors (misalignment) of the system's transmitter-receiver apparatus can induce additional deterioration in FSO performances [5]-[6].

The relay assisted communications are usually recognized as practical solutions to increase data-rate, decrease energy consumption, extend coverage and provide security [7]-[9]. The unmanned-aerial-vehicles (UAVs) can be even used as relays to assist the FSO communication systems [10]-[11]. Indeed, amplify-and forward relay (AFR) technique has an important role in cascaded FSO, RF-FSO and mmWave-FSO relay systems [12]-[14] and it is usually the case that multi-hop fading signals can be modeled as the product of two or more random processes (RPs) [15]-[21]. In particular, gamma-gamma (gg) RP can precisely address FSO links subjected to moderate to strong turbulence induced (TI) fading [22]-[24]. The analytical results for PDF of gg RP that fit well with simulations are provided in [23]. Moreover, [24] shows that for moderate to strong TI fading conditions, the gg distribution provides a good fit to the experiments for TI fluctuations collected by determined dimension of apertures related to coherence radius. Further, survey on gg RP and its application to various wireless communication systems (WCSs) as well as relay WCSs, including FSO AFR communications is presented in [25]. The paper [26] considers dual-hop AFR FSO systems over gg TI fading channels and provide closed form first order statistical results expressed mainly in terms of Fox's H and Meijer's G functions. Moreover, the first-order outage statistics such as outage probability and average bit error rate (BER) of multi-hop ASR FSO communications over gg TI fading are considered in [27]. The experimental verification of obtained results for BER of multi-hop FSO links over gg TI fading for up to 3-hop AFR FSO links are presented in [28]-[29]. In paper [30], gg TI fading model is applied for FSO link of SIM-FSO communication system.

In addition to the first order outage statistics (outage probability, bit error rate, channel

capacity and others), higher order statistics (level crossing rate - LCR and average fade duration - AFD) can reveal additional insights of time-variant fading channels. Moreover, one of the 5G requirements is ultra-reliable low-latency communications (URLLC) which is dependent on evaluation of system's outage in respect to time. In particular, the LCR indeed addresses time variant fading channels, by determining time rate of change of the output signal, while AFD is characterized as the average time for which the SNR is below a specified threshold. Thus, second order statistics can be useful for delay estimation of reliable communication links over fading channels [31]-[32]. The theoretical results for AFD and LCR of gamma-gamma RP are provided in [33]. The identical second order measures with application to FSO, verified by experiments for moderate to strong TI fading conditions are considered in [34]. Moreover, [34] has showed that analytical results are accurate with experimental results for TI fluctuations only collected by determined dimension of apertures related to coherence radius. The higher order statistics of an FSO optical link in so called Malaga TI fading conditions is then investigated in [35]. The paper [36] gives some experimental and simulation results for LCR and AFD of FSO communications. The paper [37] addresses burst error rate of time-variant FSO link over gg TI fading model, while [38] investigates security issues of FSO links over time-variant gg TI fading channels. However, the above mention references as well as the references within do not consider the second order statistics of *N*-hop AFR FSO systems over moderate to strong TI fading conditions. The closed form analytical expressions for second order statistics derived by Laplace integration formula (LIF) of mixed triple-hop RF-FSO-RF over gg TI fading model for FSO link are given in [16]. Moreover, the LIF can be often useful for application in the performance analysis of wireless communication systems [16]-[21], [39]. The LIF and exponential LIF are characterized by its generality and simplicity of application and can be used to provide closed form precise approximations that can significantly decrease computational time of complex, many-folded integral expressions [40]-[42].

To summarize, the gg is one of the most used FSO channel models for moderate to strong TI fading conditions [25]-[30], [36]-[38] that has been verified by experimental and simulation results [23]-[24], [34]. Since *N*-gg channel model can address *N*-hop AFR FSO communications in moderate to strong TI fading conditions [27], we rely on *N*-gg channel model for the second order performance analysis of *N*-hop AFR FSO communications. Other FSO channel models that are available in literature are: log-normal TI fading model (mainly

used under weak TI fading conditions) [15], double generalized gamma TI fading model (applicable for weak to strong TI conditions but there aren't available experimental validations for TI fading conditions) [43], general Malaga TI channel model (applicable for weak to strong TI fading conditions but there aren't available experimental validations for TI fading conditions, especially regarding the second order statistics) [35] and exponential-generalized gamma TI fading model (applicable for underwater optical wireless communications) [44].

Motivation of this work is to investigate the impact of the number of relays under moderate and strong TI fading conditions in relation to second the order statistics of *N*-hop AFR FSO system. In particular, significance of this paper is mathematical framework development for derivation of closed form expressions such as *i*.) PDF, *ii*.) CDF, *iii*.) LCR and *iv*.) AFD expressions of the products of i.n.i.d *N* gg RPs by direct application of LIF and exponential LIF. The obtained results are then related to the system performance of *N*-hop AFR FSO communications over gg TI fading. Moreover, the impact of moderate and strong TI fading conditions as well as the number of hops on the second order statistics of the proposed model are well investigated, numerically evaluated and presented.

To the best of author's knowledge there is no paper on the second order statistics of *N*-gg RP approximated by LIF and exponential LIF that are directly related to the *N*-hop AFR FSO system over moderate to strong TI fading conditions.

2. Gamma-gamma channel model

The gg model is based on the assumption that the fluctuations of the received optical signals, which were formed during the transmission through the turbulent FSO channel, can be modeled as a product of $x_{gg,1}$ and $x_{gg,2}$ RPs, where these two processes originate from eddies of large and small dimensions, respectively. It is assumed that $x_{gg,1}$ and $x_{gg,2}$ are statistically independent RPs. Thus, we can express the gg RP as:

$$z_{gg} = x_{gg,1}x_{gg,2} \tag{1}$$

The large-scale and small-scale TI fluctuations are described by gamma PDFs [23, eq. (10)] and [23, eq. (11)], respectively:

$$p_{X_{gg,1}}(x_{gg,1}) = \frac{\alpha^{\alpha}}{\Gamma(\alpha)}(x_{gg,1})^{\alpha-1}e^{-\alpha x_{gg,1}}, x_{gg,1} > 0, \alpha > 0; \tag{2}$$

$$p_{X_{gg,2}}(x_{gg,2}) = \frac{\beta^{\beta}}{\Gamma(\beta)}(x_{gg,2})^{\beta-1}e^{-\beta x_{gg,2}}, x_{gg,2} > 0, \beta > 0; \tag{3}$$

where α and β are large-scale and small-scale cells related to atmospheric TI fading conditions [22]-[24], respectively. The PDF of gg RP, as already given in [23, eq. (13)], is:

$$p_{z_{gg}}(z_{gg}) = \frac{2(\alpha\beta)^{\frac{\alpha+\beta}{2}}}{\Gamma(\alpha)\Gamma(\beta)}(z_{gg})^{\frac{\alpha+\beta}{2}-1}K_{\alpha-\beta}[2(\alpha\beta z_{gg})^{1/2}] \tag{4}$$

The PDF of double Nakagami-m squared (dNs) can be written as:

$$z_{dNs} = {x_{n,1}}^2{x_{n,2}}^2 \tag{5}$$

where PDFs of Nakagami-m are given as [48, eq. (2.52)]:

$$p_{x_{n,i}}(x_{n,i}) = \frac{2(m_i/\Omega_i)^{m_i}}{\Gamma(m_i)}(x_{n,i})^{2m_i-1}e^{-\frac{m_i}{\Omega_i}(x_{n,i})^2}, i = 1, 2; \tag{6}$$

The PDF of dNs can be expressed as:

$$p_{Z_{dNs}}(z_{dNs}) = \int_0^{\infty}\left|\frac{dx_{n,1}}{dz_{dNs}}\right| p_{X_{n,1}}\left(\frac{{z_{dNs}}^{1/2}}{x_{n,2}}\right)p_{X_{n,2}}(x_{n,2})dx_{n,2} \tag{7}$$

where $\left|\frac{dx_{n,1}}{dz_{dNs}}\right| = \frac{1}{2}\frac{{z_{dNs}}^{1/2}}{x_{n,2}}$. After substitution (6) in (7) and after some mathematical transformations, the $p_{Z_{dNs}}(z_{dNs})$, can be written as:

$$p_{Z_{dNs}}(z_{dNs}) = \frac{2\left(\frac{m_1m_2}{\Omega_1\Omega_2}\right)^{\frac{m_1+m_2}{2}}}{\Gamma(m_1)\Gamma(m_2)}(z_{dNs})^{\frac{m_1+m_2}{2}-1}K_{m_1-m_2}[2(\frac{m_1m_2}{\Omega_1\Omega_2}z_{dNs})^{1/2}] \tag{8}$$

Since the gamma RPs can be expressed as Nakagami-m squared RPs ($x_{gg,1} = {x_{n,1}}^2$ and $x_{gg,2} = {x_{n,2}}^2$) [48, eq. (2.55)] and where for the set of parameters: $m_1 = \alpha$, $m_2 = \beta$ and $\Omega_1 = \Omega_2 = 1$, $p_{Z_{dNs}}(z_{dNs})$ given by (8) reduces to $p_{\mathrm{z_{gg}}}(\mathrm{z_{gg}})$ given by (4), it is obvious that manipulation with gg PDF or dNs PDF for determined set of parameters should lead to the same results. Manipulation with the same RP can be more tractable but also useful in some AFR scenarios, especially in mixed RF-FSO, where for example RF propagation environment

can be modeled with Nakagami-m and FSO propagation environment can be modeled with the product of two Nakagami-m squared RPs [16].

3. N-gamma-gamma channel model for N-hop relaying

The most often applied relaying protocols for FSO or mixed RF-FSO relaying schemes are amplify-and-forward relays (AFRs) as well as decode-and-forward relays (DFRs) [12]-[13], [45]. The DFR systems can usually provide better results than AFR systems in terms of performance metrics but due to relatively lower complexity AFR systems are often proposed for application in practice [12]-[13], [28]-[29], [39], [46]. In [46], the authors compare AFR and DFR systems and propose hybrid system in order to improve the system performance, consisting of both AFRs and DFRs.

The cascaded fading channels can be modeled as the product of RPs [15]-[19], [27], [47]. It has been shown by [19, eq. (39)] that the total fading signal amplitude without AWGN at destination node of AFR channel can be modeled as the product of N Rayleigh RPs, where for the case of semi-blind, fixed gain AFRs, the gain is given by [19, eq. (52)]. In [47], the part of the system that includes dual-hop AFR channel is modeled as the product of double Gaussian RPs and the channel gain [47, eq. (2)], where the channel gain is given as a constant scaling factor equal to one in numerical results. Moreover, the FSO multi-hop transmissions by considering TI fading channels under weak TI fading conditions are given entirely as a product of log-normal RPs [15, eq. (13)]. The first order statistics of FSO multi-hop AFR system over gg RPs is presented in [27], where the overall TI fading gain is given by [27, eq. (26)].

The TI fading signal of a FSO link in moderate to strong fading conditions can be modeled using gamma-gamma (gg) random process (RP) [22]-[24]. The *N*-hop AFR communication system over gg TI fading channels is presented in Fig. 1.

We model TI fading signal at the output of *N*-hop FSO amplify-and-forward relaying AFR from source (S) laser to destination (D) reception apparatus through *N-1* number of relays (R1, R2…RN-1) as the product of *N* i.n.i.d gg RPs multiplied by channel gain G_i for each hop.

$$z_{gg,AFR}(t) = \prod_{i=1}^{N} G_i z_{gg,i}(t), i = 1, N; \tag{9}$$

According to [48, eq. (2.55)], the gamma RP can be expressed as squared Nakagami-m RP. Thus, we express the gg RP as the product of two independent but not necessarily identically distributed (i.n.i.d) Nakagami-m squared RPs for each of *N* number of hops:

$$z_{gg,out} = \prod_{i=1}^{N} z_{gg,i} = \prod_{i=1}^{N} {x_{n,i1}}^2 {x_{n,i2}}^2 \tag{10}$$

where the total output TI fading signal is denoted as $z_{gg,out}$. The TI fading signal at the output of $\underline{i}$-th hop is denoted as $z_{gg,i}\ i = 1, N$ and ${x_{n,i1}}^2 {x_{n,i2}}^2, i = 1, N$ is the product of two squared Nakagami-m RPs of *i*-th hop.

Similarly, as in [27], under the assumption that the TI fading amplitude of the product of N gg RPs can be estimated at reception without necessity for being estimated at the output of each hop, the instantaneous end-to-end SNR at the destination node can be considered as the cascaded one and can be modeled as the product of N i.n.i.d squared gg RPs. Accordingly, the instantaneous end-to-end SNR at destination node of FSO N-hop AFR system denoted as γ_{AFR} is presented as in [27, eq. (27)]:

$$\gamma_{AFR} = \frac{E_{sym}}{N_O} \prod_{i=1}^{N} {G_i - 1}^2 {z_{gg,i}}^2, i = 1, N; \tag{11}$$

where E_{sym} presents the mean energy of the transmitted symbols and N_O presents the overall noise power at the destination node. The ${G_0}^2 = 1$ and ${G_i}^2\ i = 1,\ N - 1$ for the fixed gain FSO AFR links over gg TI fading channels are already calculated and given by [27, eq. (30)]. The PDF of Nakagami-m is given as [48, eq. (2.52)]:

$$p_{x_{n,ij}}(x_{n,ij}) = \frac{2(m_{ij}/\Omega_{ij})^{m_{ij}}}{\Gamma(m_{ij})} (x_{n,ij})^{2m_{ij}-1} e^{-\frac{m_{ij}}{\Omega_{ij}}(x_{n,ij})^2}, i = 1, N; j = 1,2; \tag{12}$$

The gg RPs for FSO transmission over strong to moderate TI fading conditions are observed for normalized average powers, $\Omega_{ij} = 1, i = 1, N; j = 1, 2;$ [22]-[24]. The large-scale cells (denoted as α_i) and small-scale cells (denoted as β_i) related to atmospheric TI fading conditions of *i*-th link are [22]-[24], respectively,

$$\alpha_i = m_{i1} = [exp\left(\frac{0.49{\delta_i}^2}{\left(1 + 0.18{d_i}^2 + 0.56{\delta_i}^{12/5}\right)^{7/6}}\right) - 1]^{-1} \tag{13}$$

$$\beta_i = m_{i2} = [exp\left(\frac{0.51{\delta_i}^2 (1 + 0.69{\delta_i}^{12/5})^{-5/6}}{\left(1 + 0.9{d_i}^2 + 0.62{d_i}^2{\delta_i}^{12/5}\right)^{5/6}}\right) - 1]^{-1}, \tag{14}$$

where, ${\delta_i}^2 = 0.5 C_{n_i}^2 {k_i}^{7/6} {L_i}^{11/6}$ is the Rytov variance and $d_i = \sqrt{k_i {D_i}^2 / 4L_i}$ is the optical wave number of *i*-th link. Further, ${C_{n_i}}^2$ is Refractive index, $k_i = 2\pi/\lambda_i$ is wave-number (λ_i-wavelength), D_i is receiver aperture diameter and L_i is propagation distance of *i*-th link. The FSO AFR system model parameters used throughout text are summarized in Table I.

TABLE I. FSO SYSTEM MODEL PARAMETERS

System parameters	Definition
$\alpha_i = m_{i1}$	large-scale cells related to atmospheric conditions of *i*-th link
$\beta_i = m_{i2}$	small-scale cells related to atmospheric conditions of *i*-th link
${\delta_i}^2$	Rytov variance of *i*-th link
${C_{n_i}}^2$	Refractive index of *i*-th link (range: $10^{-17} m^{-2/3}$ to $10^{-13}\ m^{-2/3}$)
k_i	wave-number of *i*-th link
λ_i	wavelength of *i*-th link
D_i	receiver aperture diemeter of *i*-th link
L_i	optical distance of *i*-th link
${\sigma_{gg,i}}^2$	Gamma-gamma irradiance variance of *i*-th link
$v_{0,i}$	quasi frequency of *i*-th link
ut_i	average wind speed of *i*-th link

The FSO AFR system abbreviations used throughout the text are summarized in Table II.

TABLE II. FSO AFR SYSTEM ABBREVIATIONS

Abbreviations	Definition
AFD	Average fade duration
AFR	Amplify and forward relay
AWGN	Additive white Gaussian noise
B5G	Beyond 5th generation
BER	Bit error rate
CDF	Cumulative distribution function
DFR	Decode and forward relay
FSO	Free space optics
gg	Gamma-gamma
i.n.i.d	independent but not necessarily identically distributed
LCR	Level crossing rate

Abbreviations	Definition
LIF	Laplace integration formula
PDF	Probability density function
RP	Random Process
RF	Radio frequency
SIM	Subcarrier intensity modulation
SNR	Signal to noise ratio
TI	Turbulence induced
UAV	Unmanned aerial vehicle
URLLC	Ultra-reliable low-latency communications
G	Gaussian
WCS	Wireless communication systems
5G	5th Generation

4. PDF and CDF of *N*-gamma-gamma channel model

The PDF of $z_{gg,out}$ can be obtained by solving (2N-1)-folded integral according to [48]-[50]:

$$p_{z_{gg,out}}(z_{gg,out}) = \int_0^\infty dx_{n,12} \int_0^\infty dx_{n,21} \dots \int_0^\infty dx_{n,N1} \int_0^\infty \left|\frac{dx_{n,11}}{dz_{gg,out}}\right| p_{x_{n,11}}\left(\frac{{z_{gg,out}}^{\frac{1}{2}}}{x_{n,12}x_{n,21}\dots x_{n,N1}x_{n,N2}}\right) \cdot p_{x_{n,12}}(x_{n,12})p_{x_{n,21}}(x_{n,21})p_{x_{n,22}}(x_{n,22})\dots p_{x_{n,N1}}(x_{n,N1})p_{x_{n,N2}}(x_{n,N2})dx_{n,N2} \quad (15)$$

where $\left|\frac{dx_{n,11}}{dz_{gg,out}}\right| = \frac{\frac{1}{2}{z_{gg,out}}^{-\frac{1}{2}}}{x_{n,12}x_{n,21}x_{n,22}\dots x_{n,N1}x_{n,N2}}$. After substitutions (13) and (14) in (12), and (12) in (15), respectively, PDF of $z_{gg,out}$ becomes:

$$p_{z_{gg,out}}(z_{gg,out}) = \frac{2^{2N-1}{\alpha_1}^{a_1}{\beta_1}^{b_1}}{\Gamma(a_1)\Gamma(b_1)} \frac{{\alpha_2}^{a_2}{\beta_2}^{b_2}}{\Gamma(a_2)\Gamma(b_2)} \dots \frac{{\alpha_N}^{a_N}{\beta_N}^{b_N}}{\Gamma(a_N)\Gamma(b_N)} {z_{gg,out}}^{\alpha_1-1} I_1 \quad (16)$$

where, I_1 is (2N-1)-folded integral expression given as:

$$I_1 = \int_0^\infty dx_{n,12} \int_0^\infty dx_{n,21} \int_0^\infty dx_{n,22} \dots \int_0^\infty dx_{n,N1} \int_0^\infty {x_{n,12}}^{2\beta_1-2\alpha_1-1} {x_{n,21}}^{2\alpha_2-2\alpha_1-1} \dots {x_{n,N2}}^{2\beta_N-2\alpha_1-1} \cdot e^{-\alpha_1\frac{z_{gg,out}}{{x_{n,12}}^2{x_{n,21}}^2{x_{n,22}}^2\dots{x_{n,N1}}^2{x_{n,N2}}^2} - \beta_1{x_{n,12}}^2 - \alpha_2{x_{n,21}}^2 \dots - \alpha_N{x_{n,N1}}^2 - \beta_N{x_{n,N2}}^2} dx_{n,N2} \quad (17)$$

The evaluation of I_1 by exponential LIF is provided in Appendix. The CDF of $z_{gg,out}$ is expressed using [48, eq. (1.41)], [51, eq. (3.381.1)], [51, eq. (8.352.1)] and [51, eq. (3.471.9)], respectively for the case where α_1 is integer:

$$F_{z_{gg,out}}(z_{gg,out}) = \int_0^{z_{gg,out}} p_{z_{gg,out}}(r)dr$$

$$= \frac{2^{2N-1}{\beta_1}^{b_1}{\alpha_2}^{a_2}{\beta_2}^{b_2}}{\Gamma(a_1)\Gamma(b_1)\Gamma(a_2)\Gamma(b_2)} \dots \frac{{\beta_N}^{b_N}}{\Gamma(b_N)}(\alpha_1 - 1)! \left(\frac{\Gamma(b_1)\Gamma(a_2)\dots\Gamma(b_N)}{2^{2N-1}{\beta_1}^{b_1}{\alpha_2}^{a_2}\dots{\beta_N}^{b_N}} - \sum_{k=0}^{a_1-1} \frac{\left(a_1 z_{gg,out}\right)^k}{k!} I_2 \right) \tag{18}$$

where, I_2 is (2N-1)-folded integral given as:

$$I_2 = \int_0^{\infty} dx_{n,12} \int_0^{\infty} dx_{n,21} \dots \int_0^{\infty} dx_{n,N1} \int_0^{\infty} {x_{n,12}}^{2\beta_1-2k-1} {x_{n,21}}^{2\alpha_2-2k-1} \dots {x_{n,N2}}^{2\beta_N-2k-1}$$

$$\cdot e^{-\alpha_1 \frac{z_{gg,out}}{{x_{n,12}}^2{x_{n,21}}^2{x_{n,22}}^2\dots{x_{n,N1}}^2{x_{n,N2}}^2} - \beta_1{x_{n,12}}^2 - \alpha_2{x_{n,21}}^2 \dots - \alpha_N{x_{n,N1}}^2 - \beta_N{x_{n,N2}}^2} dx_{n,N2} \tag{19}$$

The closed form CDF of $z_{gg,out}$ can be obtained by evaluation of I_2 using exponential LIF whose derivation is given in Appendix.

5. LCR and AFD of *N*-gamma-gamma channel model

The LCR for a given TI fading signal threshold $z_{th,gg,out}$ can be expressed as an integral of the product of the first derivative of $z_{gg,out}$ denoted as $\dot{z}_{gg,out}$ and the joint PDF of $z_{gg,out}$ and $\dot{z}_{gg,out}$ [48, eq. (12.25)]:

$$N_{z_{gg,out}}(z_{th,gg,out}) = \int_0^{\infty} \dot{z}_{gg,out}\, p_{z_{gg,out}\dot{z}_{gg,out}}(z_{th,gg,out}, \dot{z}_{gg,out}) d\dot{z}_{gg.out} \tag{20}$$

where, $p_{z_{gg,out}\dot{z}_{gg,out}}(z_{gg,out}, \dot{z}_{gg,out})$ can be obtained by averaging joint PDF of i.n.i.d RPs, $z_{gg,out}, \dot{z}_{gg,out}, x_{n,12} \dots, x_{n,N1}$ and $x_{n,N2}$ [19, eq. (12)]:

$$p_{z_{gg,out}\dot{z}_{gg,out}}(z_{gg,out}, \dot{z}_{gg,out})$$
$$= \int_0^{\infty} dx_{n,12} \int_0^{\infty} dx_{n,21} \dots \int_0^{\infty} p_{z_{gg,out}\,\dot{z}_{gg,out}\,x_{n,12}\dots\,x_{n,N2}}(z_{gg,out}\,\dot{z}_{gg,out}\,x_{n,12}\,\dots x_{n,N2})\, dx_{n,N2} \tag{21}$$

where, $p_{z_{gg,out}\,\dot{z}_{gg,out}\,x_{n,12}\dots\,x_{n,N2}}(z_{gg,out}\,\dot{z}_{gg,out}\,x_{n,12}\,\dots\,x_{n,N2})$ can be obtained by well-established mathematical framework based on joint and conditional PDFs [19, eq. (13)]:

$$p_{z_{gg,out}\,\dot{z}_{gg,out}\,x_{n,12}\dots\,x_{n,N2}}(z_{gg,out}\,\dot{z}_{gg,out}\,x_{n,12}\,\dots x_{n,N2}) = p_{\dot{z}_{gg,out}|z_{gg,out}x_{n,12}\dots\,x_{n,N2}}(\dot{z}_{gg,out}|z_{gg,out}x_{n,12}\dots\,x_{n,N2})$$

$$\cdot p_{z_{gg,out}|x_{n,12}x_{n,21}\dots\ x_{n,N2}}(z_{gg,out}|x_{n,12}x_{n,21}\dots x_{n,N2})p_{x_{n,12}}(x_{n,12})p_{x_{n,21}}(x_{n,21})\dots p_{x_{n,N2}}(x_{n,N2}) \quad (22)$$

where after simple transformations, $p_{z_{gg,out}|x_{n,12}x_{n,21}\dots x_{n,N1}\ x_{n,N2}}(z_{gg,out}|x_{n,12}x_{n,21}\dots x_{n,N2})$ is:

$$p_{z_{gg,out}|x_{n,12}x_{n,21}\dots x_{n,N2}}(z_{gg,out}|x_{n,12}x_{n,21}\dots x_{n,N2}) = \left|\frac{x_{n,11}}{dz_{gg,out}}\right| p_{x_{n,11}}\left(\frac{z_{gg,out}^{\frac{1}{2}}}{x_{n,12}x_{n,21}x_{n,22}\dots x_{n,N2}}\right) \quad (23)$$

After substitutions, (23) in (22), (22) in (21) and (21) in (20), respectively, the $N_{z_{gg,out}}(z_{th,gg,out})$ becomes:

$$N_{z_{gg,out}}(z_{th,gg,out}) = \int_0^\infty dx_{n,12}\int_0^\infty dx_{n,21}\dots\int_0^\infty dx_{n,N1}\int_0^\infty dx_{n,N2}\left|\frac{x_{n,11}}{dz_{gg,out}}\right| p_{x_{n,11}}\left(\frac{z_{th,gg,out}^{\frac{1}{2}}}{x_{n,12}x_{n,21}x_{n,22}\dots x_{n,N1}x_{n,N2}}\right)$$

$$\cdot p_{x_{n,12}}(x_{n,12})p_{x_{n,21}}(x_{n,21})\dots p_{x_{n,N2}}(x_{n,N2})\int_0^\infty \dot{z}_{gg,out}\, p_{\dot{z}_{gg,out}|z_{th,gg,out}x_{n,12}\dots\ x_{n,N2}}(\dot{z}_{gg,out}|z_{gg,out}x_{n,12}\ \dots\ x_{n,N2})d\dot{z}_{gg.out} \quad (24)$$

The integral of the product of $\dot{z}_{gg,out}$ and conditional pdf of $\dot{z}_{gg,out}$ is:

$$\int_0^\infty \dot{z}_{gg,out}\, p_{\dot{z}_{gg,out}|z_{gg,out}x_{n,12}\dots\ x_{n,N1}\ x_{n,N2}}(\dot{z}_{gg,out}|z_{gg,out}x_{n,12}\ \dots\ x_{n,N2})d\dot{z}_{gg,out} = \frac{1}{\sqrt{2\pi}}\sigma_{\dot{z}_{gg,out}} \quad (25)$$

where the $\sigma^2_{\dot{z}_{gg,out}}$ is the variance of $\dot{z}_{gg,out}$. Since the first derivative of zero mean Gaussian (G) RP is G RP and the linear transformation of the G RPs is zero mean G RP, the $\dot{z}_{gg,out}$ is thus zero mean G RP and can be expressed as:

$$\dot{z}_{gg,out} = \dot{z}_{gg,1}\ for\ N = 1$$
$$\dot{z}_{gg,out} = z_{gg,2}z_{gg,3}\dots z_{gg,N}\dot{z}_{gg,1} + z_{gg,1}z_{gg,3}\dots z_{gg,N}\dot{z}_{gg,2}\dots + z_{gg,1}z_{gg,2}\dots z_{gg,N-1}\dot{z}_{gg,N},\ for\ N > 1 \quad (26)$$

After mathematical transformation of $z_{gg,i} = {x_{n,i1}}^2{x_{n,i2}}^2, i = 1, N$, the $\sigma^2_{\dot{z}_{gg,out}}$ as a zero mean G RP can be expressed through the variances of $z_{gg,1}, z_{gg,2}\ \dots\ z_{gg,N}$, denoted as $\sigma^2_{\dot{z}_{gg,1}}, \sigma^2_{\dot{z}_{gg,2}}\dots\sigma^2_{\dot{z}_{gg,\mathrm{N}}}$, respectively,

$$\sigma^2_{\dot{z}_{gg,out}} = \sigma^2_{\dot{z}_{gg,1}}, for\ N = 1$$
$$\sigma^2_{\dot{z}_{gg,out}} = \sigma^2_{\dot{z}_{gg,1}}{x_{n,21}}^4{x_{n,22}}^4\dots{x_{n,N2}}^4\left(1 + \frac{{z_{gg,out}}^2\sigma^2_{\dot{z}_{gg,2}}/\sigma^2_{\dot{z}_{gg,1}}}{{x_{n,21}}^8{x_{n,22}}^8{x_{n,31}}^4{x_{n,32}}^4\dots{x_{n,N1}}^4{x_{n,N2}}^4}\right.$$
$$+\frac{{z_{gg,out}}^2\sigma^2_{\dot{z}_{gg,3}}/\sigma^2_{\dot{z}_{gg,1}}}{{x_{n,21}}^4{x_{n,22}}^4{x_{n,31}}^8{x_{n,32}}^8\dots{x_{n,N1}}^4{x_{n,N2}}^4}\dots$$
$$\left.+\frac{{z_{gg,out}}^2\sigma^2_{\dot{z}_{gg,N}}/\sigma^2_{\dot{z}_{gg,1}}}{{x_{n,21}}^4{x_{n,22}}^4{x_{n,31}}^4{x_{n,32}}^4\dots{x_{n,N1}}^8{x_{n,N2}}^8}\right), for\ N > 1 \quad (27)$$

Finally, by substituting (27) in (25) and then (12) and (25) in (24), we obtained (2N-1)-folded integral expression for LCR for a given threshold $z_{TH,gg,out}$ over N-gg RP, given as:

$$N_{z_{gg,out}}(z_{TH,gg,out}) = \frac{2^{2N-1}{\alpha_1}^{a_1}{\beta_1}^{b_1}}{\sqrt{2\pi}\,\Gamma(a_1)\Gamma(b_1)} \frac{{\alpha_2}^{a_2}{\beta_2}^{b_2}}{\Gamma(a_2)\Gamma(b_2)} \dots \frac{{\alpha_N}^{a_N}{\beta_N}^{b_N}}{\Gamma(a_N)\Gamma(b_N)} {z_{TH,gg,out}}^{\alpha_1-1} I_3 \tag{28}$$

where, I_3 is (2N-1)-folded integral expressed as:

$$I_3 = \int_0^\infty dx_{n,12} \int_0^\infty dx_{n,21} \dots \int_0^\infty dx_{n,N1} \int_0^\infty \sigma_{\dot{z}_{gg,out}} \tag{29}$$
$$\cdot {x_{n,12}}^{2\beta_1-2\alpha_1-1} {x_{n,21}}^{2\alpha_2-2\alpha_1-1} \dots {x_{n,N2}}^{2\beta_N-2\alpha_1-1} e^{-\alpha_1 \frac{z_{TH,gg,out}}{{x_{n,12}}^2 {x_{n,21}}^2 {x_{n,22}}^2 \dots {x_{n,N2}}^2} - \beta_1 {x_{n,12}}^2 - \alpha_2 {x_{n,21}}^2 \dots - \alpha_N {x_{n,N1}}^2 - \beta_N {x_{n,N2}}^2} dx_{n,N2}$$

The closed form derivation by LIF for $N_{z_{TH,gg,out}}(z_{TH,gg,out})$ is presented in the Appendix. We close this section with derivation of average fade duration (AFD) for a given TI fading threshold $z_{TH,gg,out}$ of N-gg RP as:

$$AFD(z_{TH,gg,out}) = \frac{F_{z_{gg,out}}(z_{TH,gg,out})}{N_{z_{gg,out}}(z_{TH,gg,out})} = \frac{\sqrt{2\pi}(\alpha_1-1)! \left(\frac{\Gamma(b_1)\Gamma(a_2)\dots\Gamma(b_N)}{2^{2N-1}{\beta_1}^{b_1}{\alpha_2}^{a_2}\dots{\beta_N}^{b_N}} - \sum_{k=0}^{a_1-1} \frac{\left(a_1 z_{TH,gg,out}\right)^k}{k!} I_2 \right)}{{\alpha_1}^{a_1} {z_{TH,gg,out}}^{\alpha_1-1} I_3} \tag{30}$$

where I_2 and I_3 are integral expressions in terms of $z_{TH,gg,out}$, already obtained in (19) and (29), respectively. Closed form mathematical development for AFD$(z_{TH,gg,out})$ is also presented in Appendix.

6. Numerical Results

In this section we present some numerical results for second order statistics of *N*-hop FSO AFR system over gg TI fading channels.

The N-hop FSO AFR end-to-end link is modeled with N-gg distribution, where numerical results are computed for various optical fading severity parameters (α_i, $\beta_i, i = 1, N$) and various gg irradiance variances (${\sigma_{gg,i}}^2 = \frac{1}{\alpha_i} + \frac{1}{\beta_i} + \frac{1}{\alpha_i \beta_i}$) [22]-[24]. The $\sigma^2_{\dot{Z}_{gg,i}}, i = 1, N$ in (27) are zero mean Gaussian (G) RPs assumed to take the same value, $\sigma^2_{\dot{Z}_{gg}} = \sigma^2_{\dot{Z}_{gg,i}} = {v_{0,i}}^2 \pi^2 {\sigma_{gg,i}}^2 \langle Z_i \rangle$, as given in [35, eq. (13)], where we take the normalized $\langle Z_i \rangle = 1$ for gg RP. Moreover, the $v_{0,i}$ is so called quasi frequency of the *i*-th link specified as the frequency of fades when output signal is equal to received signal light [34]-[35] and can be further expressed as $v_{0,i} = \frac{1}{\pi \tau_{0,i} \sqrt{2}}$ [35, eq. (15)]. Furthermore, $\tau_{0,i} = \frac{\sqrt{\lambda_i L_i}}{u t_i}$ is turbulence correlation time of i-th link, where λ_i is optical window, L_i is optical distance and $u t_i$ is average wind

speed of *i*-th FSO link [35].

The paper [15] provides the impact of the number of hops on second order statistics for weak TI fading conditions of multi-hop FSO system. In order to explore moderate and strong TI fading conditions we consider that all links of *N*-hop FSO AFR system are exposed to moderate $(\alpha = \alpha_i = 5.42,\ \beta = \beta_i = 3.8)$ or strong $(\alpha = \alpha_i = 4,\ \beta = \beta_i = 1.71)$ fading conditions. The TI fading parameters are summarized in Table III.

TABLE III. TI FADING PARAMETERS FOR MODERATE AND STRONG TI FADING CONDITIONS

Turbulence	$\alpha = \alpha_i$	$\beta = \beta_i$	${C_n}^2 = {C_{n_i}}^2$
Moderate Turbulence	5.42	3.8	$3 \cdot 10^{-14} m^{-2/3}$
Strong Turbulence	4	1.71	$1 \cdot 10^{-13} m^{-2/3}$

Without loss of generality, we assume the system setting parameters of each *i*-th link of *N*-hop FSO AFR end-to-end system $(\lambda = \lambda_i = 1550nm,\ ut = ut_i = \frac{10m}{s}, L = L_i = 1000m)$ are as in [35].

Fig. 2 reports the behavior of $N_{z_{gg,out}}(z_{TH,gg,out})$ in moderate and strong TI fading conditions for various numbers of links at the output of *N*-hop AFR FSO end-to-end communications. Comparison between LIF approximate results and results derived from exact analytical integral expression shows that the matching for observed system parameters is well achieved, especially for higher output threshold dB values. The one-hop FSO communications over gg RP, especially for moderate TI fading conditions provides the lowest $N_{z_{gg,out}}(z_{TH,gg,out})$ values for the whole range of $z_{TH,gg,out}$. It can be seen that by shifting from strong to moderate TI fading conditions, $N_{z_{gg,out}}(z_{TH,gg,out})$ decreases, as expected. Moreover, we observe the impact of different number of hops (for example N=1, N=2 and N=4) on $N_{z_{gg,out}}(z_{TH,gg,out})$. It can be concluded that increase in number of hops leads to increase in $N_{z_{gg,out}}(z_{TH,gg,out})$ for the same TI fading conditions and is expected to increase further for higher number of hops. It is also evident that the impact of TI fading severities on $N_{z_{gg,out}}(z_{TH,gg,out})$ are more dominant in lower $z_{TH,gg,out}$ dB regime while the number of hops are more dominant in higher $z_{TH,gg,out}$ dB regime on $N_{z_{gg,out}}(z_{TH,gg,out})$ for the proposed model and for the observed system model parameters. It can be seen that in lower $z_{TH,gg,out}$ dB regime, the $N_{z_{gg,out}}(z_{TH,gg,out})$ has lower values due to the increased

probability of signal envelope being below $z_{TH,gg,out}$. It can be further noticed that at the value around 0~1 dB of $z_{TH,gg,out}$, $N_{z_{gg,out}}(z_{TH,gg,out})$ has higher values due to increased probability of signal envelope shifting from below to above $z_{TH,gg,out}$ level and vice versa. At this point, $N_{z_{gg,out}}(z_{TH,gg,out})$ is mainly independent of TI fading conditions and the number or relays. Moreover, in higher $z_{TH,gg,out}$ dB regime the $N_{z_{gg,out}}(z_{TH,gg,out})$ has again lower values due to the increased probability of signal envelope being above $z_{TH,gg,out}$.

The behavior of AFD$(z_{TH,gg,out})$ is shown in Fig. 3. Shifting from strong to moderate TI fading conditions leads to AFD$(z_{TH,gg,out})$ decrease for lower $z_{TH,gg,out}$ dB values while AFD$(z_{TH,gg,out})$ increase for higher $z_{TH,gg,out}$ dB values. Fig. 3 is presented from -10 dB to 20 dB since in that range behavior of AFD$(z_{TH,gg,out})$ in relation to system model parameters can be well observed and fitting between exact and approximative AFD$(z_{TH,gg,out})$ can be determined. Below this range approximation for AFD$(z_{TH,gg,out})$ fails to follow the behavior of exact AFD$(z_{TH,gg,out})$. One need to have in mind that moderate TI fading is assumed to be $(\alpha = 5,\ \beta = 3.8)$ since α must be integer in (18). Similar trend is noticeable with the increase of the number of hops. Namely, with increase in the number of hops, AFD$(z_{TH,gg,out})$ increases for lower $z_{TH,gg,out}$ while decreases for higher $z_{TH,gg,out}$ values.

It can be noticed that at the value around 0~1 dB of $z_{TH,gg,out}$, $N_{z_{gg,out}}(z_{TH,gg,out})$ and AFD$(z_{TH,gg,out})$ are independent of TI fading conditions and the number of relays.

Fig. 4 provides $N_{z_{gg,out}}(z_{TH,gg,out})$ behavior of dissimilar TI fading conditions of *N*-hop FSO AFR system. It can be seen that in the case of higher number of links, moderate TI fading conditions and lower N can cause $N_{z_{gg,out}}(z_{TH,gg,out})$ to decrease. $AFD(z_{TH,gg,out})$ in dissimilar TI fading conditions of *N*-hop FSO AFR system is presented in Fig 5.

The $N_{z_{gg,out}}$ versus N (number of hops) under different TI fading conditions and for different $z_{TH,gg,out}$ is presented in Fig. 6. It can be noticed that increasing of observed $z_{TH,gg,out}$ can decrease not only $N_{z_{gg,out}}$ but also the impact between moderate and strong TI fading conditions. Moreover, the observed numerical results suggest that selection of adequate $z_{TH,gg,out}$ can diminish the impact between moderate and strong TI fading conditions for the observed number of hops. Fig. 7 provides the AFD versus N (number of hops) under moderate and strong TI fading conditions and for different $z_{TH,gg,out}$. It can be

concluded that increasing number of hops for N-hop AFR FSO communications can diminish the impact between moderate and strong TI fading conditions for the observed $z_{TH,gg,out}$.

By comparing obtained results for $N_{z_{gg,out}}(z_{TH,gg,out})$ and $AFD(z_{TH,gg,out})$ with available results in the literature [15]-[16], [19], [31]-[35] similar behavior in relation to the number of hops and fading severity parameters can be noticed. Moreover, the obtained results in [28]-[29] indicate that higher number of hops can improve performances in terms of BER and Ergodic Capacity. On the other hand, the [15] shows that increase in number of hops for multi-hop FSO communications can provide AFD to increase for observed parameters, as has been shown for lower $z_{TH,gg,out}$ values in Figure 3.

TABLE IV. SYSTEM PERFORMANCES EXECUTION TIME

System Performance	$N_{z_{gg,out}}(z_{TH,gg,out})$			AFD$(z_{TH,gg,out})$		
Number of Relays	N=1	N=2	N=4	N=1	N=2	N=4
Execution Time in sec. (Exact)	0.328125	114.906	1180.95	0.453125	771.203	4584.36
Execution Time in sec. (App.)	0.015625	0.018625	0.03125	0.0625	0.046875	0.28125

Table IV presents execution time of exact and approximative $N_{z_{gg,out}}(z_{TH,gg,out})$ and AFD$(z_{TH,gg,out})$ expressions in Wolfram MATHEMATICA for the range from -20dB to 20dB. It can be observed, that execution time of exact expressions takes much more time than execution time of closed form approximative expressions.

7. Conclusion

In this paper, the second-order statistics of the N-hop FSO AFR link over gg TI fading channels are considered. A LIF and exponential LIF based mathematical approach have been applied for derivation of approximate closed-form expressions for *i.)* PDF, *ii.)* CDF, *iii.)* LCR and *iv.)* AFD. The CDF and AFD expressions are valid only for an integer value of α_1, since those expressions are dependent on the finite sum expression that goes from zero to $\alpha_1 - 1$. Moreover, comparisons of exact, integral-form analytical expressions and LIF based approximated, fast-computing, closed-form expressions of $N_{z_{gg,out}}(z_{TH,gg,out})$ and AFD$(z_{TH,gg,out})$ for moderate and strong TI fading conditions and for different number of hops are provided. The system performance improvement is evident by shifting from strong to moderate TI fading conditions, especially for the lower $z_{TH,gg,out}$ dB values. The increasing number of relays leads to increase in $N_{z_{gg,out}}(z_{TH,gg,out})$ for all $z_{TH,gg,out}$ values under the same TI fading conditions and increase in AFD$(z_{TH,gg,out})$ for

lower $z_{TH,gg,out}$ values under the same TI fading conditions. Thus, the number of relays can indeed impact the system performances in time-variant TI fading channels. One can conclude that multi-hop FSO link design needs to take into account the number of hops on second-order statistics in order to achieve the best performances. Our future works are envisioned to include experimental and simulation verification of the results on the second order statistics on *N*-hop AFR FSO systems over gg TI fading channels. Moreover, the pointing errors and DFRs are also envisioned to be included in the future results.

Appendix

The system is modeled with the product of 2N random variables $\prod_{i=1}^{N} {x_{n,i1}}^2 {x_{n,i2}}^2, i = 1, N$; resulting in (2N-1)-folded analytical integral expressions for $p_{z_{gg,out}}(z_{gg,out})$, $F_{z_{gg,out}}(z_{gg,out})$, $N_{z_{gg,out}}(z_{TH,gg,out})$ and AFD$(z_{TH,gg,out})$, already presented in (16), (18), (28) and (30), respectively. The (2N-1)-folded integrals can be solved by direct application of general LIF [19, eq. (I.3)], given as:

$$\int_0^\infty dx_{n,12} \int_0^\infty dx_{n,21} \dots \int_0^\infty dx_{n,N1} \int_0^\infty f_1(x_{n,12}, x_{n,21}, \dots x_{n,N1}, x_{n,N2})\, e^{-\gamma f_2(x_{n,12}, x_{n,21}, \dots x_{n,N1}, x_{n,N2})} dx_{n,N2}$$

$$\approx \left(\frac{2\pi}{\gamma}\right)^{\frac{2N-1}{2}} \frac{f_1\left(x_{n,12}(0), x_{n,21}(0) \dots, x_{n,N2}(0)\right)}{\sqrt{deth}} e^{-\gamma f_2\left(x_{n,12}(0), x_{n,21}(0), \dots, x_{n,N2}(0)\right)} \tag{31}$$

where $x_{n,12}(0), x_{n,21}(0) \dots, x_{n,N2}(0)$ are obtain from the set of differential equations, respectively,

$$\left.\begin{aligned} \frac{\partial f_2\left(x_{n,12}(0), x_{n,21}(0) \dots, x_{n,N2}(0)\right)}{\partial x_{n,12}(0)} &= 0 \\ \frac{\partial f_2\left(x_{n,12}(0), x_{n,21}(0) \dots, x_{n,N2}(0)\right)}{\partial x_{n,21}(0)} &= 0 \\ \vdots & \\ \frac{\partial f_2\left(x_{n,12}(0), x_{n,21}(0) \dots, x_{n,N2}(0)\right)}{\partial x_{n,N2}(0)} &= 0 \end{aligned}\right\} \tag{32}$$

whereas, h is Hessian matrix given as:

$$h = \begin{vmatrix} \frac{\partial^2 f_2(x_{n,12}(0) \dots x_{n,N2}(0))}{\partial x_{n,12}(0)^2} & \frac{\partial^2 f_2(x_{n,12}(0) \dots x_{n,N2}(0))}{\partial x_{n,12}(0) \partial x_{n,21}(0)} & \dots & \frac{\partial^2 f_2(x_{n,12}(0) \dots x_{n,N2}(0))}{\partial x_{n,12}(0) \partial x_{n,N2}(0)} \\ \frac{\partial^2 f_2(x_{n,12}(0) \dots x_{n,N2}(0))}{\partial x_{n,21}(0) \partial x_{n,12}(0)} & \frac{\partial^2 f_2(x_{n,12}(0) \dots x_{n,N2}(0))}{\partial x_{n,21}(0)^2} & \dots & \frac{\partial^2 f_2(x_{n,12}(0) \dots x_{n,N2}(0))}{\partial x_{n,21}(0) \partial x_{n,N2}(0)} \\ \vdots & \vdots & & \vdots \\ \frac{\partial^2 f_2(x_{n,12}(0) \dots x_{n,N2}(0))}{\partial x_{n,N2}(0) \partial x_{n,12}(0)} & \frac{\partial^2 f_2(x_{n,12}(0) \dots x_{n,N2}(0))}{\partial x_{n,N2}(0) \partial x_{n,21}(0)} & \dots & \frac{\partial^2 f_2(x_{n,12}(0) \dots x_{n,N2}(0))}{\partial x_{n,N2}(0)^2} \end{vmatrix} \tag{33}$$

The complexity of LIF based mathematical approach for derivation of closed form analytical approximate expressions increase with the number of RPs (for instance by modelling N-hop AFR over gg TI fading channels as a product of 2N-Nakagami-m squared RPs, we need to solve (2N-1)-folded integrals for $p_{z_{gg,out}}(z_{gg,out})$, $F_{z_{gg,out}}(z_{gg,out})$, $N_{z_{gg,out}}(z_{TH,gg,out})$ and AFD$(z_{TH,gg,out})$. This can be done by using software package Mathematica and by applying appropriate algorithm that can be efficiently used in practice. Moreover, LIF based mathematical method can significantly decrease computational time if compared to integral form analytical expressions.

Appendix A
Closed form PDF derivation

Approximate closed form $p_{z_{gg,out}}(z_{gg,out})$ is obtained from (16) by solving I_1 in (17), using exponential LIF for the following set of functions**:**

$$\gamma = 1$$

$$f_1\left(x_{n,12}(0), x_{n,21}(0) \dots x_{n,N2}(0)\right) = 1$$

$$f_2\left(x_{n,12}(0), x_{n,21}(0) \dots x_{n,N2}(0)\right) = \frac{\alpha_1 z_{gg,out}}{x_{n,12}(0)^2 x_{n,21}(0)^2 \dots x_{n,N2}(0)^2} + \beta_1 x_{n,12}(0)^2 + \alpha_2 x_{n,21}(0)^2 \dots + \beta_N x_{n,N2}(0)^2$$
$$-(2\beta_1 - 2\alpha_1 - 1)\, ln\left(x_{n,12}(0)\right) - (2\alpha_2 - 2\alpha_1 - 1)\, ln\left(x_{n,21}(0)\right) \dots - (2\beta_N - 2\alpha_1 - 1)\, ln\left(x_{n,N2}(0)\right) \quad (34)$$

where I_1 in (17) is expressed as a fully exponential function by applying simple transformation:

$$x_{n,12}{}^{2\beta_1 - 2\alpha_1 - 1} x_{n,21}{}^{2\alpha_2 - 2\alpha_1 - 1} \dots x_{n,N2}{}^{2\beta_N - 2\alpha_1 - 1} = e^{(2\beta_1 - 2\alpha_1 - 1)\, ln(x_{n,12}) + (2\alpha_2 - 2\alpha_1 - 1)\, ln(x_{n,21}) \dots + (2\beta_N - 2\alpha_1 - 1)\, ln(x_{n,N2})} \quad (35)$$

After solving (32) for the particular $f_2\left(x_{n,12}(0), x_{n,21}(0) \dots x_{n,N2}(0)\right)$ from (34) and after substitutions of (33) and (34) in (31), the I_1 in (17) can be obtained and substituted in (16) for derivation of closed form expression for $p_{z_{gg,out}}(z_{gg,out})$.

Appendix B
Closed form CDF derivation

Similarly, approximate closed form expression for $F_{z_{gg,out}}(z_{gg,out})$ is obtained from solving integral I_2 in (18) and substituting in (19), using exponential LIF for the following arguments:

$$\gamma = 1$$

$$f_1\left(x_{n,12}(0), x_{n,21}(0) \dots x_{n,N2}(0)\right) = 1$$

$$f_2\left(x_{n,12}(0), x_{n,21}(0) \dots x_{n,N2}(0)\right) = \frac{\alpha_1 z_{TH,gg,out}}{x_{n,12}(0)^2 x_{n,21}(0)^2 \dots x_{n,N2}(0)^2} + \beta_1 x_{n,12}(0)^2 + \alpha_2 x_{n,21}(0)^2 \dots + \beta_N x_{n,N2}(0)^2$$
$$-(2\beta_1 - 2k - 1)\, ln\left(x_{n,12}(0)\right) - (2\alpha_2 - 2k - 1)\, ln\left(x_{n,21}(0)\right) \dots - (2\beta_N - 2k - 1)\, ln\left(x_{n,N2}(0)\right) \quad (36)$$

where we used simple transformation in (19):

$$x_{n,12}{}^{2\beta_1 - 2k - 1} x_{n,21}{}^{2\alpha_2 - 2k - 1} \dots x_{n,N2}{}^{2\beta_N - 2k - 1} = e^{(2\beta_1 - 2k - 1)\, ln\left(x_{n,12}\right) + (2\alpha_2 - 2k - 1)\, ln\left(x_{n,21}\right) \dots + (2\beta_N - 2k - 1)\, ln\left(x_{n,N2}\right)} \quad (37)$$

After calculating (32) for $f_2\left(x_{n,12}(0), x_{n,21}(0) \dots x_{n,N2}(0)\right)$ from (36) and after some mathematical derivations and substitutions of (33) and (36) in (31), I_2 in (19) is solved and substituted in (18) for derivation of closed form expression for $F_{z_{gg,out}}(z_{gg,out})$.

Appendix C
Closed form second order statistics derivation

The approximate $N_{z_{gg,out}}(z_{TH,gg,out})$ of N-gg RP is solved form (28) by applying LIF in (29) for the functions:

$$\gamma = 1$$

$$f_1\left(x_{n,12}(0), x_{n,21}(0) \dots, x_{n,N2}(0)\right) = 1, \qquad N = 1$$

$$f_1\left(x_{n,12}(0), x_{n,21}(0) \dots, x_{n,N2}(0)\right)$$
$$= \left(1 + \frac{z_{TH,gg,out}{}^2 \sigma^2_{\dot{Z}_{n,2}} / \sigma^2_{\dot{Z}_{n,1}}}{x_{n,21}{}^8 x_{n,22}{}^8 x_{n,31}{}^4 x_{n,32}{}^4 \dots x_{n,N1}{}^4 x_{n,N2}{}^4} + \frac{z_{TH,gg,out}{}^2 \sigma^2_{\dot{Z}_{n,3}} / \sigma^2_{\dot{Z}_{n,1}}}{x_{n,21}{}^4 x_{n,22}{}^4 x_{n,31}{}^8 x_{n,32}{}^8 \dots x_{n,N1}{}^4 x_{n,N2}{}^4} \dots \right.$$
$$\left. + \frac{z_{TH,gg,out}{}^2 \sigma^2_{\dot{Z}_{n,N}} / \sigma^2_{\dot{Z}_{n,1}}}{x_{n,21}{}^4 x_{n,22}{}^4 x_{n,31}{}^4 x_{n,32}{}^4 \dots x_{n,N1}{}^8 x_{n,N2}{}^8}\right)^{1/2}, \qquad N > 1 \quad (38)$$

$$f_2\left(x_{n,12}(0), x_{n,21}(0) \dots x_{n,N2}(0)\right) = \frac{\alpha_1 z_{TH,gg,out}}{x_{n,12}(0)^2 x_{n,21}(0)^2 \dots x_{n,N2}(0)^2} + \beta_1 x_{n,12}(0)^2 + \alpha_2 x_{n,21}(0)^2 \dots + \beta_N x_{n,N2}(0)^2$$
$$-(2\beta_1 - 2\alpha_1 - 1)\, ln\left(x_{n,12}(0)\right) - (2\alpha_2 - 2\alpha_1 + 1)\, ln\left(x_{n,21}(0)\right) \dots - (2\beta_N - 2\alpha_1 + 1)\, ln\left(x_{n,N2}(0)\right)$$

where we use similar transformation in (29):

$$x_{n,12}{}^{2\beta_1-2\alpha_1-1}x_{n,21}{}^{2\alpha_2-2\alpha_1+1}\dots x_{n,N2}{}^{2\beta_N-2\alpha_1+1} = e^{(2\beta_1-2\alpha_1-1)\,ln(x_{n,12})+(2\alpha_2-2\alpha_1+1)\,ln(x_{n,21})\dots+(2\beta_N-2\alpha_1+1)\,ln(x_{n,N2})} \quad (39)$$

The approximate closed form $N_{z_{gg,out}}(z_{TH,gg,out})$ is derived from (28) by evaluating I_3 in (29), where after calculating (32) for this particular case and after appropriate substitutions of (33) and (38) in (31). Finally, $AFD(z_{TH,gg,out})$ is derived as approximate closed form expression as the ratio of approximate closed form expressions for $F_{z_{gg,out}}(z_{gg,out})$ and $N_{z_{gg,out}}(z_{TH,gg,out})$.

Acknowledgments

Caslav Stefanovic would like to acknowledge CONEX-Plus project. The CONEX-Plus has received research funding from UC3M and the European Union's Horizon 2020 programme under the Marie Skłodowska-Curie grant agreement No 801538. The authors would like to thank Editor and anonymous Reviewers for their valuable comments that significantly improved the paper quality. The authors would like to acknowledge the COST Action 16220.

References

1. M. Alzenad, M. Z. Shakir, H. Yanikomeroglu, M. S. Alouini, "FSO-based vertical backhaul/fronthaul framework for 5G+ wireless networks", *IEEE Communications Magazine*, vol. 56, no. 1, pp. 218-224, 2018.
2. E. Yaacoub, M. S. Alouini. "A key 6G challenge and opportunity--connecting the remaining 4 billions: A Survey on Rural Connectivity", *arXiv preprint arXiv*:1906.11541, 2019.
3. S. Song, Y. Liu, L. Guo, Q. Song, "Optimized relaying and scheduling in cooperative Free Space Optical fronthaul/backhaul of 5G", *Optical Switching and Networking*, vol. 30, pp. 62-70. 2018.
4. A. S. Hamza, J. S. Deogun, D. R. Alexander, "Classification framework for free space optical communication links and systems", *IEEE Communications Surveys & Tutorials*, vol. 21, no. 2, pp. 1346-1382, 2018.
5. L. Yang, X. Gao, M. S. Alouini, "Performance analysis of relay-assisted all-optical FSO networks over strong atmospheric turbulence channels with pointing errors", *Journal of Lightwave Technology*, vol. 32, no. 23, pp. 4613-4620, 2014.
6. D. Nace, M. Pióro, M. Poss, F. D'Andreagiovanni, I. Kalesnikau, M. Shehaj, A. Tomaszewski, "An optimization model for robust FSO network dimensioning" *Optical Switching and Networking*, vol. 32, pp. 25-40, 2019.
7. K. R. Liu, A. K. Sadek, W. Su, A. Kwasinski, "Cooperative communications and networking" Cambridge university press, 2009.
8. H. Hu, H. Yanikomeroglu, D. D. Falconer, S. Periyalwar, "Range extension without capacity penalty in cellular networks with digital fixed relays", *In IEEE Global Telecommunications Conference, 2004. GLOBECOM'04,* Vol. 5, pp. 3053-3057, 2004.

9. F. Jameel, S. Wyne, G. Kaddoum, T. Q. Duong, "A comprehensive survey on cooperative relaying and jamming strategies for physical layer security", *IEEE Communications Surveys & Tutorials*, vol. 21, no. 3, pp. 2734-2771, 2018.
10. M. T. Dabiri, S. M. S. Sadough, M. A. Khalighi, "Channel modeling and parameter optimization for hovering UAV-based free-space optical links", *IEEE Journal on Selected Areas in Communications*, vol. 36, no. 9, pp. 2104-2113, 2018.
11. P. Zhu, J. Zhang, Z. Gao, L. Bai, Y. Ji "Adaptive resource allocation in FSO/RF multiuser system with proportional fairness for UAV application. *Optical Switching and Networking*, *33*, 41-48, 2019.
12. K. P. Peppas, A. N. Stassinakis, H. E. Nistazakis, G. S. Tombras, "Capacity analysis of dual amplify-and-forward relayed free-space optical communication systems over turbulence channels with pointing errors." *IEEE/OSA Journal of Optical Communications and Networking* vol. 5, no. 9, pp.1032-1042, 2013.
13. S. Anees, M. R. Bhatnagar, "Performance of an amplify-and-forward dual-hop asymmetric RF–FSO communication system", Journal of Optical Communications and Networking, vol. 7, no. 2, pp. 124-135, 2015.
14. Y. Zhang, J. Zhang, L. Yang, B. Ai, M. S. Alouini, "On the Performance of Dual-Hop Systems over Mixed FSO/mmWave Fading Channels", *IEEE Open Journal of the Communications Society*, vol. 1, pp. 477-489, 2020.
15. C. B. Issaid, M. S. Alouini. "Level Crossing Rate and Average Outage Duration of Free Space Optical Links", *IEEE Transactions on Communications*, vol. 67, no. 9, pp. 6234-6242, 2019.
16. C. Stefanovic, M. Pratesi, F. Santucci "Second Order Statistics of Mixed RF-FSO Relay Systems and its Application to Vehicular Networks", IEEE ICC'19 ONF Symposium, Shangai, China, May 20- May 24, 2019.
17. N. Hajri, R. Khedhiri, N. Youssef, "On Selection Combining Diversity in Dual-Hop Relaying Systems Over Double Rice Channels: Fade Statistics and Performance Analysis", *IEEE Access*, vol. 8, pp. 72188-72203, 2020.
18. N. Zlatanov, Z. Hadzi-Velkov, G. K. Karagiannidis, "Level crossing rate and average fade duration of the double nakagami-m random process and application in MIMO keyhole fading channels, " IEEE Communications Letters, vol. 12, no. 11, pp. 822 – 824, Nov. 2008.
19. Z. Hadzi-Velkov, N. Zlatanov, G. K. Karagiannidis, "On the second order statistics of the multihop rayleigh fading channel", IEEE Transactions on Communications, vol. 57, no. 6, pp 1815 – 1823, 2009.
20. N. Milosevic, M. Stefanovic, Z. Nikolic, P. Spalevic, C. Stefanovic, "Performance analysis of interference-limited mobile-to-mobile κ–μ fading channel." *Wireless Personal Communications*, vol. 101, no. 3, pp. 1685-1701, 2018.
21. N. Milosevic, C. Stefanovic, Z. Nikolic, M. Bandjur, M. Stefanovic. "First-and second-order statistics of interference-limited mobile-to- mobile Weibull fading channel." *Journal of Circuits, Systems and Computers* 2018, vol. 27, no. 11, 2018.
22. L. C. Andrews, R. L. Phillips, Laser beam propagation through random media, SPIE Press, 2nd edition, 2005.
23. A. Al-Habash, L. C. Andrews, R. L. Phillips, "Mathematical model for the irradiance probability density function of a laser beam propagating through turbulent media," *Optical engineering*, vol. 40*,* no. 8, pp. 1554-1563, 2001.
24. F. S. Vetelino, C. Young, L. C. Andrews, J. Recolons, "Aperture averaging effects on the probability density of irradiance fluctuations in moderate-to-strong turbulence," *Applied Optics*, vol. 46, no. 11, pp. 2099–2108, Apr. 2007.
25. S. Al-Ahmadi, "The gamma-gamma signal fading model: A survey", *IEEE Antennas and Propagation Magazine,* vol*.* 56*,* no. 5, pp. 245-260, 2014.
26. E. Zedini, H. Soury, M. S. Alouini, "Dual-hop FSO transmission systems over gamma–gamma turbulence with pointing errors", *IEEE Transactions on Wireless Communications*, vol. *16*, no. 2, pp. 784-796, 2016.

27. C. K. Datsikas, K. P. Peppas, N. C. Sagias, G. S. Tombras, “Serial free-space optical relaying communications over gamma-gamma atmospheric turbulence channels:, *IEEE/OSA Journal of Optical Communications and Networking*, vol. 2, no. 8, pp. 576-586, 2010.
28. N. A. M. Nor, Z. Ghassemlooy, J. Bohata, P. Saxena, M. Komanec, S. Zvanovec, M. A., Bhatnagar, M. A. Khalighi, "Experimental investigation of all-optical relay-assisted 10 Gb/s FSO link over the atmospheric turbulence channel." *Journal of Lightwave Technology* vol. 35, no. 1, pp. 45-53, 2016.
29. N. A. M. Nor, Z. Ghassemlooy, S. Zvanovec, M. A. Khalighi, M. R. Bhatnagar, J. Bohata, M. Komanec, “Experimental analysis of a triple-hop relay-assisted FSO system with turbulence”, *Optical Switching and Networking*, vol. 33, pp. 194-198, 2019.
30. M. Petković, N. Zdravković, C. Stefanović, G. Đorđević, “Performance analysis of SIM-FSO system over Gamma-Gamma atmospheric channel”, XLIX International Scientific Conference on Information, Communication and Energy Systems and Technologies - ICEST 2014, Proceedings of papers, Nis, Serbia, vol. 1, pp. 19-22, 25-27 June 2014.
31. S. K. Yoo, S. L. Cotton, P. C. Sofotasios, S. Muhaidat, G. K. Karagiannidis, “Level Crossing Rate and Average Fade Duration in F Composite Fading Channels”, *IEEE Wireless Communications Letters*, 2019.
32. F. J. Lopez-Martinez, E. Kurniawan, R. Islam, A. Goldsmith, “Average fade duration for amplify-and-forward relay networks in fading channels”, *IEEE Transactions on Wireless Communications*, vol. 14, no. 10, pp. 5454-5467, 2015.
33. H. T. Yura and S. G. Hanson, ”Mean level signal crossing rate for an arbitrary stochastic process,” J. Opt. Soc. Am. A, vol. 27, no. 4, pp. 797-807, 2010.
34. F. S. Vetelino, C. Young, L. Andrews, “Fade statistics and aperture averaging for Gaussian beam waves in moderate-to-strong turbulence”, *Applied optics*, vol. 46, no. 18, pp. 3780-3789, 2007.
35. A. Jurado-Navas, J. M. Garrido Balsells, M Castillo-Vazquez, A. Puerta-Notario, I. T. Monroy, J. J. V. Olmos, “ Fade statistics of M-turbulent optical links”, *EURASIP Journal on Wireless Communications and Networking*, (2017) 2017:112, DOI:10.1186/s13638-0170898-z.
36. H. K. Kim, T. Higashino, K. Tsukamoto, S. Komaki, “Optical fading analysis considering spectrum of optical scintillation in terrestrial free-space optical channel”, *IEEE International Conference on Space Optical Systems and Applications*, pp. 58-66, May, 2011.
37. H. D. Le, V. V. Mai, C. T. Nguyen, A. T. Pham, “Design and analysis of sliding window arq protocols with rate adaptation for burst transmission over fso turbulence channels”, *Journal of Optical Communications and Networking*, vol. 11, no. 5, pp. 151-163, 2019.
38. X. Sun, I. B. Djordjevic, M. A. Neifeld, “Secret key rates and optimization of BB84 and decoy state protocols over time-varying free-space optical channels”, *IEEE Photonics Journal*, vol. 8, no. 3, pp. 1-13, 2016.
39. C. Stefanovic, M. Pratesi, F. Santucci, “Second order performance evaluation of cooperative communications over fading channels in vehicular networks”, Second URSI Atalntic Science Radio Meeting, 2018.
40. R. W. Butler, A. t. Wood, ”Laplace approximations for hypergeometric functions with matrix argument”, *The Annals of Statistics*, vol. 30, no. 4, pp. 1155-1177, 2002.
41. M. C. Harding, J. Hausman, “Using a Laplace approximation to estimate the random coefficients logit model by nonlinear least squares”, *International Economic Review*, vol. *48,* no. 4, pp. 1311-1328, 2007.

42. J. Wang, "Dirichlet processes in nonlinear mixed effects models", *Communications in Statistics—Simulation and Computation*, vol. 39, no. 3, pp. 539-556, 2010.
43. H. Al Quwaiee, I. S. Ansari, M. S. Alouini, "On the performance of free-space optical communication systems over double generalized gamma channel", *IEEE Journal on Selected Areas in Communications*, vol. *33*, no. 9, pp.1829-1840, 2015.
44. S. Li, L. Yang, D. B. da Costa, J. Zhang, M. S. Alouini, "Performance Analysis of Mixed RF-UWOC Dual-Hop Transmission Systems", *IEEE Transactions on Vehicular Technology*, vol. 69, no. 11, pp. 14043-14048.
45. E. Balti, M. Guizani, B. Hamdaoui, B. Khalfi, "Aggregate hardware impairments over mixed RF/FSO relaying systems with outdated CSI", *IEEE Transactions on Communications*, vol. *66*, pp. 3, pp. 1110-1123, 2017.
46. G. Levin, S. Loyka, "Amplify-and-forward versus decode-and-forward relaying: Which is better?", In *22th International Zurich seminar on communications (IZS)*, Eidgenössische Technische Hochschule Zürich, 2012.
47. B. Talha, S. Primak, M. Pätzold, "On the statistical properties of equal gain combining over mobile-to-mobile fading channels in cooperative networks" ,In *2010 IEEE International Conference on Communications* (pp. 1-6). IEEE, 2010.
48. L. G. Stüber, *Principles of mobile communication*, Vol. 2. Norwell, Mass, USA: Kluwer Academic, 1996.
49. M. K. Simon, M. S. Alouini, *Digital communication over fading channels*. Vol. 95. John Wiley & Sons, 2005.
50. C. Stefanovic, D. Djosic, S. Panic, D. Milic, M. Stefanovic, A Framework for Statistical Channel Modeling in 5G Wireless Communication Systems. 5G Multimedia communications: Technology, multiservices, deployment, CRC Press 2020, pp. 31-54, 2020.
51. I. S. Gradshteyn, I. M. Ryzhik, *Table of Integrals, Series, and Products*, 6th ed., New York: Academic, 2000.

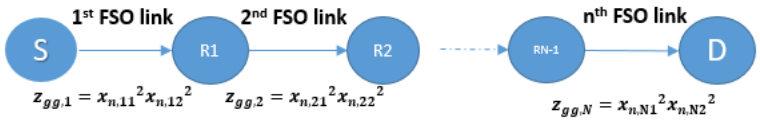

Fig. 1. Simplified model of *N*-hop amplify-and-forward relay (AFR) communication system over gg TI fading channels.

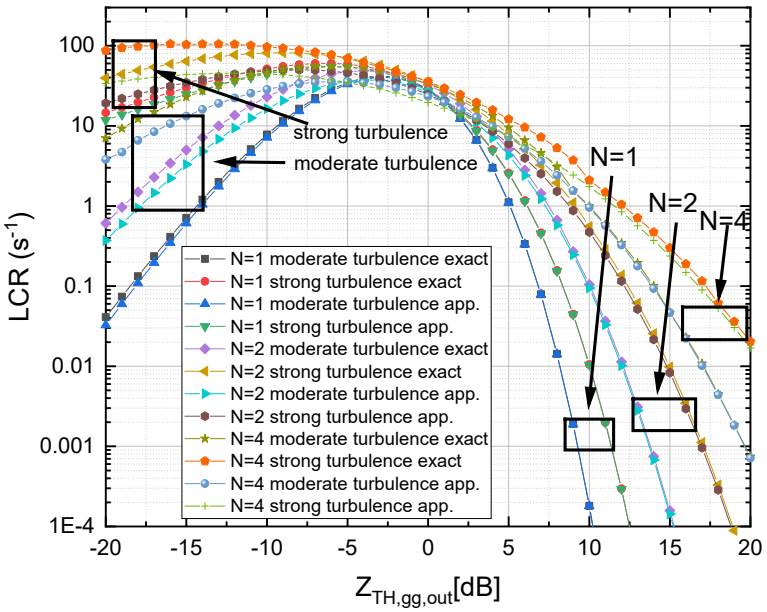

Fig. 2. LCR (s^{-1}) versus $z_{TH,gg,out}$ under different TI fading conditions and for various number of hops.

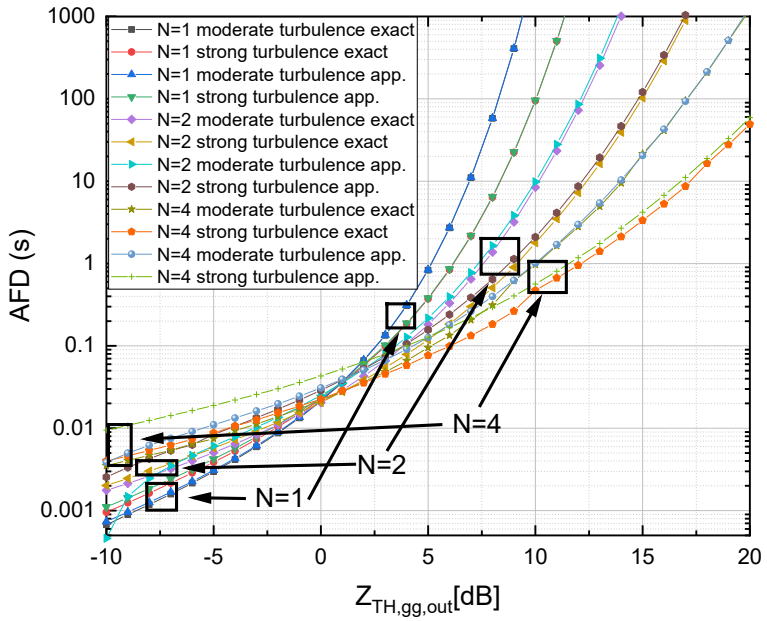

Fig. 3. AFD (s) versus $z_{TH,gg,out}$ under different TI fading conditions and for various number of hops.

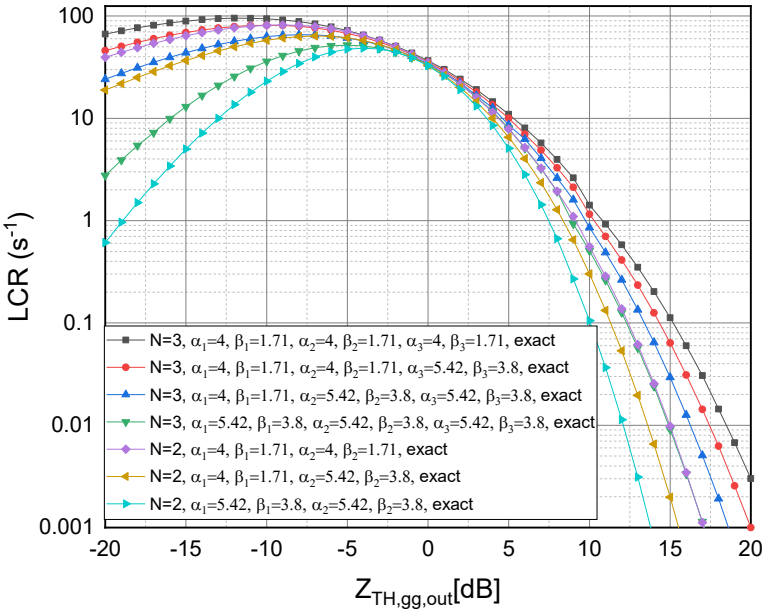

Fig. 4. LCR (s^{-1}) versus $z_{TH,gg,out}$ under dissimilar TI fading conditions and for different number of hops.

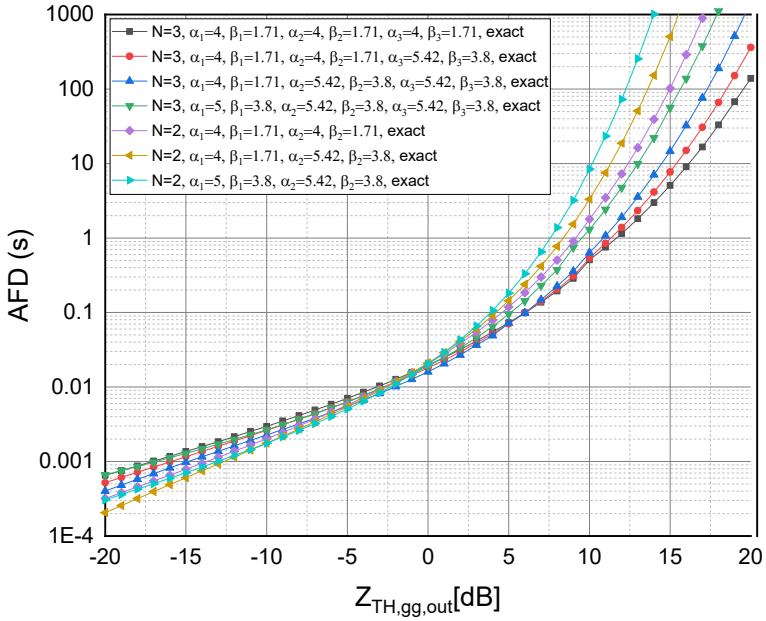

Fig. 5. AFD (s) versus $z_{TH,gg,out}$ under dissimilar TI fading conditions.

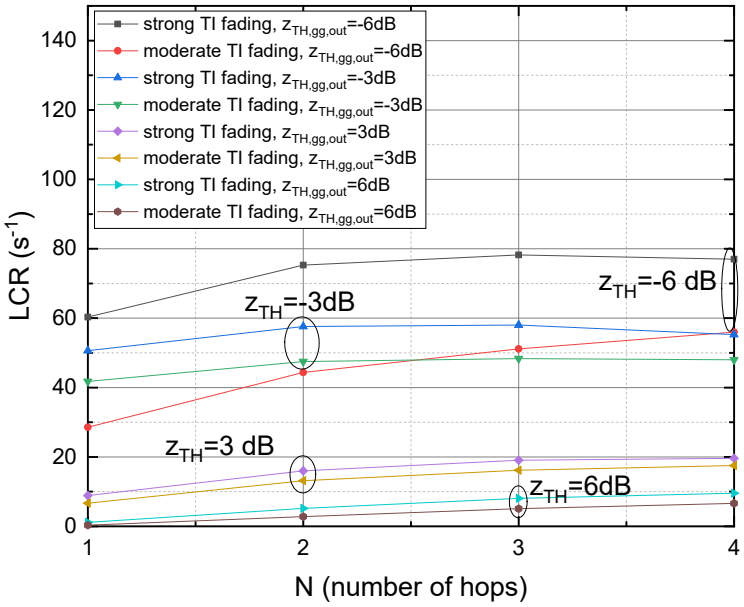

Fig. 6. LCR (s^{-1}) versus N under different TI fading conditions and for different $z_{TH,gg,out}$.

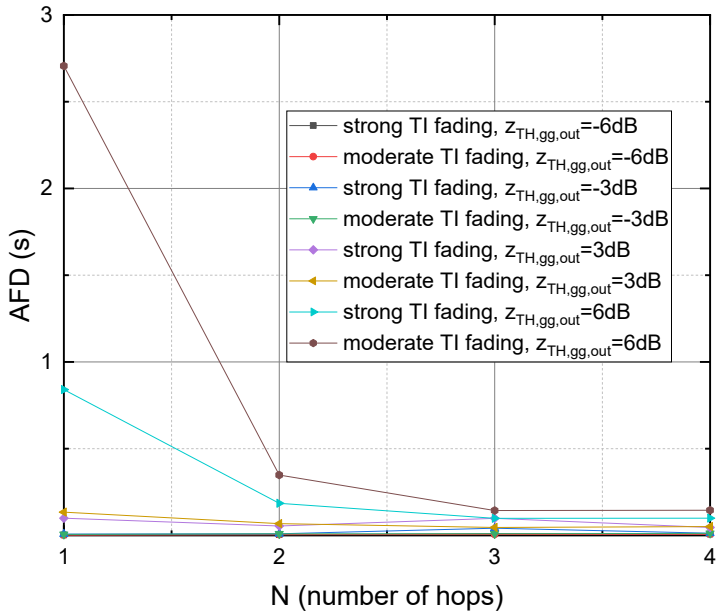

Fig. 7. AFD (s) versus N under different TI fading conditions and for different $z_{TH,gg,out}$.